UNIVERSITY OF OXFORD

XFORD ASTROPHYSICS

MAGING OF THE FIELD OF 4C41.17
BELOW THE LYMAN LIMIT

Mark Lacy and Steve Rawlings

6/1

Address: Department of Physics,
Astrophysics,
Keble Road,
Oxford,
OX1 3RH,
England.

Imaging of the field of 4C41.17 below the Lyman limit

Mark Lacy & Steve Rawlings

Astrophysics, Department of Physics, Keble Road, Oxford, OX1 3RH

17 December 1995

ABSTRACT

Imaging of $z \geq 3.4$ radio galaxy fields below the Lyman continuum wavelength allows companion galaxies to be identified on the basis of red colours across the wavelength of redshifted Lyα and very red colours across the redshifted Lyman continuum. These arise due to a combination of absorption by intervening Lyα forest and Lyman-limit systems, and intrinsic Lyman-limit breaks in the galaxy spectral energy distribution caused by an HI screen or breaks in stellar spectra. As a pilot study we have imaged the field of the $z = 3.8$ radio galaxy 4C41.17 in U, V and R with the Auxiliary Port of the WHT. We find a number of potential companion galaxies, which require confirmation *via* spectroscopy or narrow-band imaging. The Lyman-limit in the spectrum of the radio galaxy itself and its implications for the origin of the UV flux is also discussed.

Key words: galaxies: formation – galaxies: individual (4C41.17) – galaxies: active

1 INTRODUCTION

With the advent of CCD detectors with good responses in the near-UV, the technique of Lyman-limit imaging has become one of the most promising methods of finding normal galaxies (i.e. galaxies without powerful AGN) at high redshifts. Star-forming galaxies should be identifiable *via* a flat spectrum (in flux density f_ν *vs.* frequency ν) longward of Lyα, a break shortward of the Lyα wavelength caused by intervening Lyα forest clouds and a further break at the Lyman continuum wavelength (the "Lyman-limit"), due to the combination of an intrinsic continuum break of ≥ 2 (Bruzual & Charlot 1993), accumulated absorption by intervening Lyα forest clouds and the likelihood of high optical depth absorption by intervening Lyman-limit systems (Møller & Jakobsen 1990). This method has the great advantage of being relatively unaffected by dust compared to optical searches for Lyα emission from these objects. By searching for this characteristic spectral signature, suitable samples can be selected for further study *via* optical/IR spectroscopy and further broad-band imaging with the aim of estimating the star-formation rates and masses of these objects.

Previous uses of this technique have involved field samples (e.g. Guhathakurta, Tyson & Majewski 1990; Lilly, Cowie & Gardiner 1991) and a region around the quasar Q0000-263 which contains a damped Lyα system at $z = 3.4$ (Steidel & Hamilton 1992,1993). The field samples turned up no significant population of high-z objects, but the field of Q0000-263 turned out to have a large number (16 in ~ 15 arcmin^2) of potential $z > 3$ galaxies, a result which Giavalisco, Steidel & Slazay (1994) identify as the detection of a possible $z = 3.4$ cluster. Imaging of four other fields around damped absorbers (Steidel, Pettini & Hamilton 1995) find that a more typical density of Lyman-limit candidates is ≈ 0.5 arcmin^{-2} to a flux limit of $\mathcal{R} = 25$ (i.e. $R \approx 24.7$), corresponding approximately to the number expected if there is no evolution in the normal galaxy population out to $z \sim 3.5$.

We are basing our strategy on radio galaxy fields. Radio galaxies in the local Universe are identified with the most massive elliptical galaxies [with luminosities $\sim 3L_*$, where L_* is the break luminosity in the Schechter (1976) function], which at early times may have corresponded to the high peaks in the spectrum of density fluctuations. These fluctuations are expected to have roughly equal power on all scale-

lengths, with the effect that lesser peaks (which might form galaxies $\lesssim L_*$) tend to be clustered around the highest peaks, an effect often termed biassing. The radio luminosity of a radio galaxy with a given bulk power in its radio jets is also a strong function of environmental density (Rawlings 1992), creating a further bias towards radio galaxies being found in high density regions. Observational evidence for the existence of such effects comes from the high fraction of $z \sim 0.5$ radio galaxies and quasars found in clusters (Hill & Lilly 1991; Ellingson, Yee & Green 1991).

In this paper we report on a pilot study of the field of the redshift 3.8 radio galaxy 4C41.17 (Chambers, Miley & van Breugel 1990; hereafter Ch90). This well-studied system has several properties which make a study of this sort valuable. Deep imaging in K-band with the Keck Telescope (Graham et al. 1994; hereafter G94) shows up several red companion galaxies, possibly indicating the presence of a group or cluster around or in front of the radio galaxy. Imaging of the radio galaxy itself with the HST shows a high degree of correlation between the radio and optical structures (Miley et al. 1992). Detections with the JCMT (Dunlop et al. 1994) and IRAM (Chini & Krügel 1994) indicate the presence of large amounts ($10^8 - 10^9 M_\odot$) of dust, either in the galaxy itself, or in nearby objects within the 11- and 16.5-arcsec diameter beams of IRAM and the JCMT respectively.

2   OBSERVATIONS

The 4C41.17 field was observed by the William Herschel Telescope (WHT) at the $f/11$ Auxiliary Port on the nights of 1995 January 25,26 and 28. In addition a K-band observation of the part of the Auxiliary Port field not visible in the Keck image was made with IRCAM3 at the UKIRT 1995 March 24. Details of the imaging observations are shown in Table 1. (The observations made on 1995 January 26 were affected by stray light emanating from the GHRIL cage of the WHT; this had a negligible effect on the U-band observations, but added significant excess background to the V- and R-band images taken that night.) The seeing on the final R-band image was 1.4-arcsec.

Flux calibration was achieved by observing the standard stars 94401 and PG 1514+034 (Landholt 1992). A correction for colour was found necessary in R-band only due to the asymmetric profile of the Harris R filter. Airmass corrections were estimated by scaling the V-band extinction measurements made by the Carlsberg Automatic Meridian Circle according to the standard La Palma extinction curve (King 1985). A further correction was made to allow for the effects of the extinction in the Milky Way. The reddening was estimated to be $E(B - V) = 0.12$ from the map of Burstein & Heiles (1982), assuming $A_V = 3.1E(B - V)$ gave $A_V = 0.37$. Corresponding values of extinction as a function of wavelength in

U and R were calculated from the curves of Cardelli, Clayton & Mathis (1989). We also checked the 100μm map of the region made by *IRAS*; after subtraction of a comparable contribution of zodiacal light, the cirrus towards 4C41.17 had a flux of 6.2 MJysr^{-1}, corresponding to $A_V \approx 0.3 - 0.4$ assuming 18 ± 3 MJysr^{-1} per magnitude in A_V (Beichmann 1987).

3   ANALYSIS

The initial data reduction was performed in IRAF using standard routines to bias subtract and flatfield the data, and to align the U, V and R frames to within a pixel. The routine IMSURFIT was then used to fit a polynomial surface to the final images, which was then subtracted in order to remove large-scale fluctuations in the background level, mostly caused by scattered light from bright stars within the camera. The processed frames were then block averaged by five pixels in x and y to correctly sample the relatively poor seeing. The STARLINK PISA package was then used to find and classify the images on the R-band frame, to produce a finding list to define the set of objects for photometry. The total area surveyed was 1.49 arcmin^2. Aperture photometry was then performed on each of the objects detected in the R-band image using circular apertures with radii close to the source sizes found by PISA (except for the objects common to the K-selected sample of G94 which all have photometry in 3-arcsec diameter apertures). The results of this analysis are given in Table 2, and a finding chart is given in Fig. 1. The total R magnitudes were estimated by PISA using a "curve of growth" analysis (Kron 1980) are also listed in Table 2, along with an indication of whether the objects are stellar or extended on the basis of the HST image of Miley et al. (1992). In Table 3, we show our measurements and limits for the K-band selected objects of G94 undetected by PISA in our R-band image, in 3-arcsec diameter circular apertures.

We made an estimate of the completeness of, and errors in, our mini-survey by adding in gaussian objects of known magnitudes with full-width-half-maxima equal to the seeing using the ARTDATA package within IRAF, processing the frames in the same manner as the data frames, and then running PISA to recover them. These tests showed that the error in the total magnitudes of Table 2 at $R_{tot} \approx 24$ are about 0.5 mag. The completeness at this flux level is about 80 per cent, falling to 60 per cent by $R_{tot} \approx 24.4$. The errors and incompleteness are dominated by residual background fluctuations in the images.

Table 1. Imaging of the 4C41.17 field

Telescope/ configuration	Instrument/ Detector	Filter	Date	Exposure time /seconds	Seeing /arcsec	Notes
WHT Aux Port	TEK5	U'	25/1/95	14400	1.0	light cirrus
WHT Aux Port	TEK5	U	26/1/95	15300	2.0	clear
WHT Aux Port	TEK5	V	26/1/95	2700	2.0	clear; background $\approx$ 2× normal value
WHT Aux Port	TEK5	R	26/1/95	2700	2.0	clear; background $\approx$ 3× normal value
WHT Aux Port	TEK5	V	28/1/95	1800	1.6	clear
WHT Aux Port	TEK5	R	28/1/95	1800	1.6	clear
UKIRT Cass	IRCAM3	K	24/3/95	810	1.6	clear

Table 3. Magnitudes and colours of the objects listed in G94 undetected by PISA

Object No. in G94	R	ΔR	V	ΔV	U	ΔU	$R - K$	$\Delta R - K$
2	>25.6		>26.1		>25.4		>4.5	
4	>25.6		>26.1		>25.4		>4.8	
5	>25.6		>26.1		>25.4		>4.2	
6	>25.6		>26.1		>25.4		>4.4	
9	>25.6		>26.1		>25.4		>3.3	
12	>25.6		25.7	0.27	25.0	0.25	>4.8	
14	>25.6		>26.1		>25.4		>4.0	
16	25.1	0.23	25.0	0.14	>25.4		6.7	0.23
17	24.9	0.19	25.0	0.14	>25.4		3.9	0.29
18	25.5	0.33	>26.1		>25.4		6.0	0.34

Notes: G94 object 12 is object 'z' of Chambers et al. (1990). The errors include Poisson noise only (see notes to Table 2).

4 DISCUSSION

4.1 The field objects

Our field search is sensitive to galaxies in the range $z \sim 3 - 5$, i.e. from where the Lyman limit moves into the U-band until it exits the V-band, although for the reasons given in Section 1 we expect that any field objects are likely to be at a similar redshift to the radio galaxy. Apart from 4C41.17, there are several field objects which have spectral energy distributions (SEDs) consistent with high redshift galaxies. We have plotted the SEDs of these objects in Fig. 2 (a)-(f). LR4 is particularly interesting, as besides showing a strong spectral break between U and V, it also has a break across Lyα, consistent with Lyα forest absorption, and also is the only object apart from 4C41.17 in the field of G94 which shows a significant $K - K_S$ excess (corresponding perhaps to high EW [OIII]495.9/500.7 lines). Its comparative brightness, though, argues against an interpretation as a companion galaxy to 4C41.17 unless it harbours an AGN (it is even brighter in K_S, corresponding to $\approx 100 L_*$ at $z = 3.8$). LR7 is very faint, so the limit in U-band is relatively poor, making it hard to eliminate the possibility of it being at low-z. LR11 shows a strong break between V and R, and is undetected in U. LR14 is undetected in U, but its SED is very red from K to V. LR19 is a good candidate, with a possible break between V and R and a clear break between U and V, and faint in K-band. LR21 is undetected in U, but

shows no break between R and V, so is most likely to be a low-z galaxy or a star.

In the absence of spectroscopic confirmation, we cannot yet be certain that any of these candidates are at $z > 3$. Likely contaminants include cool stars and early-type galaxies at moderate redshifts (~ 0.3). Where our field overlaps the HST field of Miley et al. (1992), we can be fairly sure that we have correctly identified the stars. The only one of our Lyman-limit candidates which appears stellar in the HST image is LR6 [Fig. 2(g)], although is is still possible that it could be a reddened AGN at high-z. or a very compact galaxy. Moderate redshift early-type galaxies produce the largest contaminant problem. In Fig. 2(h) we show an early-type galaxy spectrum redshifted to 0.2,0.3 and 0.5. Clearly, at any of these redshifts the possibility of confusion with a Lyman-limit object is high, as all have very red $U - V$ colours [e.g. at $z = 0.3$, $U - V = 2.2$ for such a galaxy (Coleman, Wu & Weedman 1980)]. $V - R$ colours could help in principle, but due to Lyman forest absorption we expect our high-z galaxies to have red $V - R$ too. The best discriminant is probably the $R - K$ colour, which should be ≈ 2 for a flat-spectrum object, but 3-5 for $z = 0.2 - 0.5$ early-type galaxies (e.g. Dunlop et al. 1989). Of our Lyman-limit candidates, LR4, LR11 and LR14 all have measured $R - K > 3$, and LR19 and LR21 have limits in K which are too poor to discriminate. It is therefore likely that many of our candidates are only at moderate redshifts, although it is also possible that the high-z galaxies we are searching for are red, in which
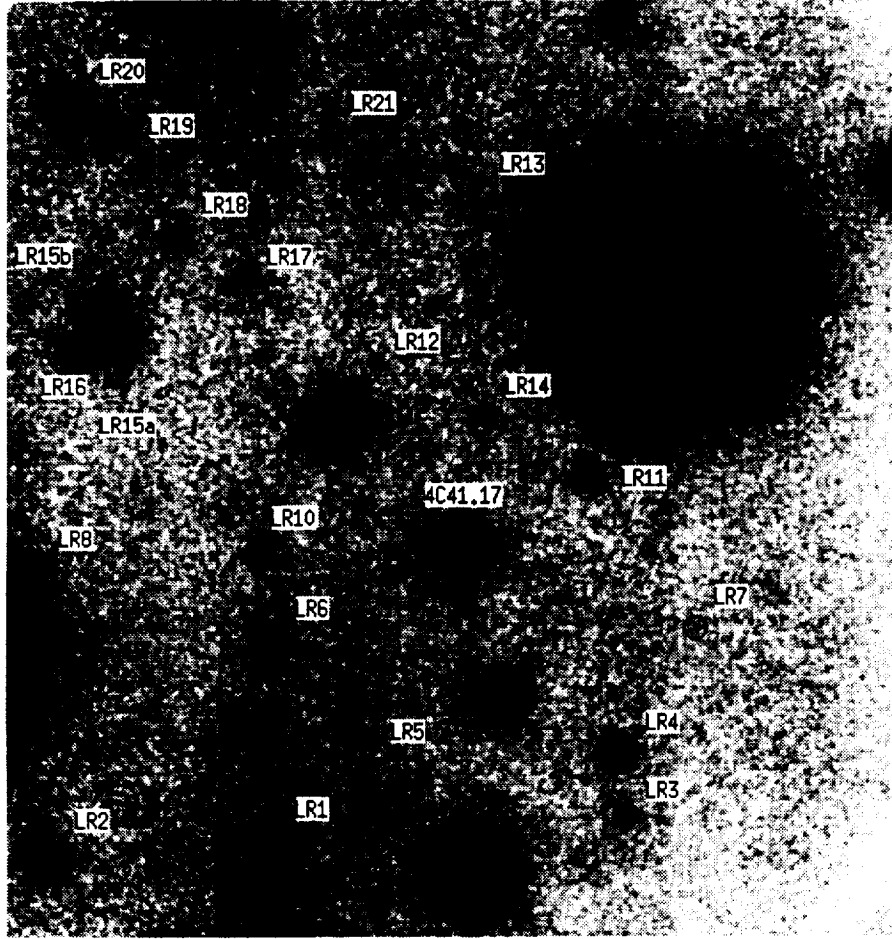
Figure 1. Finding chart for the objects listed in Table 2 made from our R-band image. The apertures used for the photometry detailed in Table 2 are shown to scale where possible, otherwise the objects are indicated by arrows. In the case of 4C41.17, the 6×4 arcsec^2 aperture of Ch90 is shown on which the points in Fig. 3 are based, in preference to the 3-arcsec diameter aperture used in Table 2. North is to the top and east to the left. The image has been smoothed with a $\sigma = 1$-pixel gaussian.

case the $R - K$ discriminant is not useful. We confirm that the very red objects detected by G94 near to the radio galaxy (G94 objects 4-6,9,12) are all plausible high-z galaxy candidates, with the exception of object 12 (object 'z' of Ch90), which is marginally detected on both our V and U-band images.

Comparing our results with those of Steidel et al. (1995), we find a somewhat higher density of Lyman limit candidates (6 in $\approx$ 1.5 arcmin^{-2}, i.e. all in Fig. 2 excluding LR21), although our selection criteria are not identical, so it is hard to make direct comparisons. It is clear though, based on the $R - K$ colours that either many of these objects are much lower redshift galaxies with early-type spectra or that the high-z galaxy population is predominately not flat spectrum,

perhaps because their epoch of maximum star formation was further back in the past. There is, however, no evidence from either the number counts of galaxies in R compared to those of Tyson (1988) or from the galaxy colours of a substantial population of unusual galaxies in this field.

4.2 The radio galaxy

There is a clear spectral break towards U-band in the SED of the radio galaxy, even after allowance has been made for the Lyα forest absorption in V-band (Fig. 3). As discussed in Møller & Jakobsen (1990) and Madau (1995), beyond the Lyman-limit strong absorption is expected from both the accumulated
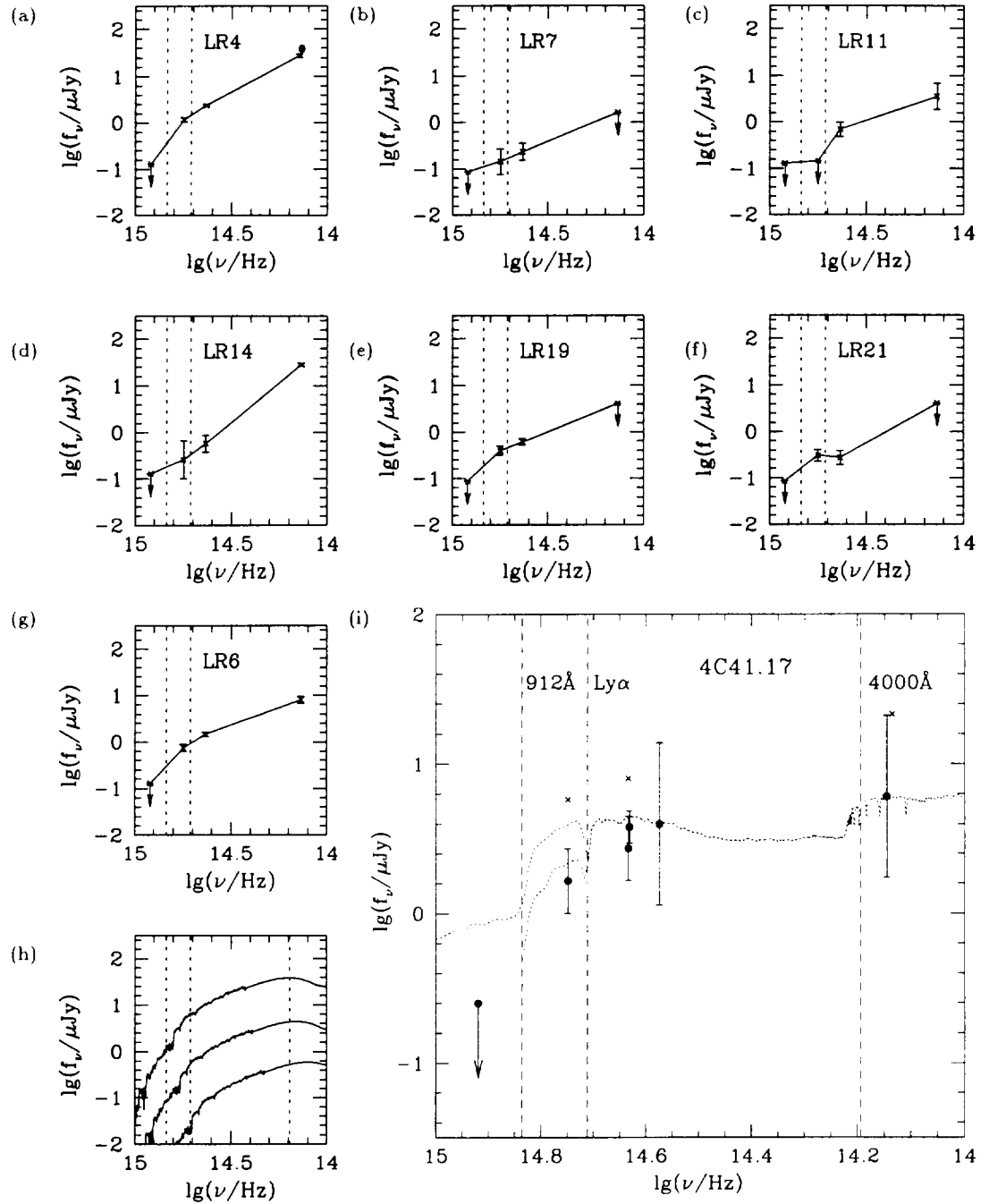
Figure 2. (a)-(g) Spectral energy distributions of the potential Lyman-limit systems. In the case of LR4, the point corresponding to the K-band magnitude is plotted as a dot and the cross is the K_s magnitude, for all the other objects the K magnitude only is plotted. The two vertical dashed lines indicate the positions of the Lyman-limit and Lyα redshifted to $z = 3.8$. (h) The "cold E/S0" SED at an age of 13 Gyr from the model of Rocca-Volmerange & Guiderdoni (1988) redshifted to $z = 0.2$ (top curve), $z = 0.3$ (middle curve) and $z = 0.5$ (bottom curve). (i) The SED of 4C41.17. Flux densities are measured in the "galaxy" 6×4 arcsec^2 aperture of Ch90. Dots represent the best estimate of the SED without lines and are from left to right U, V and R-band observations from this paper (the V and R-band observations have Lyα subtracted using the value of the Lyα flux from Ch90), line-free R-band from the HST observation of Miley et al. (1992), I-band from Ch90, and K_s-band from G94, aperture corrected by comparing the K-band magnitude of Ch90 with that of G94. The crosses represent the V, R (from this paper) and K (from G94) magnitudes including line emission. The dotted lines are correspond to a 1-Gyr burst $10^{11}M_\odot$ Bruzual model (e.g. Bruzual & Charlot 1993) after 5×10^8 yr, (i.e. a star formation rate of $100M_\odot\text{yr}^{-1}$) (top curve between 912Å and 1216Å), and (bottom curve) attenuated by median Lyman forest absorption coefficients appropriate to $z = 3.8$ estimated from fig. 9 of Warren, Hewett & Osmer (1994). Beyond the Lyman-limit, absorption is dominated by Lyman-limit systems, and is very dependent on the number of Lyman-limit systems along the line of sight, so we have not attempted to plot this.

opacity of the Lyman-limits of Lyα forest systems, and intervening Lyman-limit systems with redshifts such that they fall within the bandpass of the U filter ($z \approx 2.7 - 3.8$). Scaling from Figs. 5 and 6 of Møller & Jakobsen (1990), only 5 per cent of random lines of sight from $z = 3.8$ will have transmission $\gtrsim 10$ per cent at the rest wavelengths sampled by our U-band filter, and a typical line of sight will only have a transmission of a few per cent. This reinforces the value of Lyman-limit imaging for detecting high-z galaxies, for even if the galaxy spectrum shows only a modest Lyman-limit break, due to e.g. a very young stellar population, or radiation from supernova remnants dominating the UV light (Bithell 1991), we still expect a large observed break from intervening absorption. The corollary, however, is that Lyman-limit imaging has a restricted value for determining the UV emission mechanism in the radio galaxy itself.

Spectroscopic detections of the Lyman-limit are less likely to be confused by the presence of intervening absorbers due to the far superior wavelength resolution. For example, Storrie-Lombardi et al. (1994) find only 6/68 quasars in the range $z = 2.8 - 4.5$ with Lyman-limit systems within 4000 kms^{-1}. The disadvantage is that the wavelength dispersion makes detections at a given signal-to-noise ratio much harder. Nevertheless, a spectroscopic detection of a Lyman-limit break in 4C41.17 was reported by Dickinson, Spinrad & Liebert (1991).

An intrinsic break, if present, could have one of two physical causes; either it reflects breaks in stellar spectra (thus implying that the near-UV light is dominated by stars), or it is due to HI absorption by a screen of HI in front of the UV-emitting region of the galaxy with a column density $N(\text{HI}) \geq 1.6 \times 10^{21}$ m^{-2} (e.g. Storrie-Lombardi et al. 1994). It is hard to eliminate the possibility of the existence of such a screen, but the lack of evidence for strong absorption in the Lyα line [the Fabry-Perot observations of Hippelein & Meisenheimer (1993) detect only a low column density absorber and there is no significant velocity offset between the Lyα and [OIII]500.7 (Eales & Rawlings 1993)] argues against one being present.

In the absence of such a screen, UV light with an intrinsic Lyman-limit break is most likely to come from stars. Scattering can be ruled out provided there is a negligible amount of HI mixed in with the scatterers and there is no intrinsic break in the quasar spectrum at 912Å. Although a a dust and HI mixture would be able to create a Lyman-limit break in scattered light, this would create the same effect on the Lyα emission as an HI screen between the UV-emitting region and the Lyα halo discussed previously. An additional argument against scattering was provided by Miley et al. (1992) who noted that the close radio-optical correspondences in the HST image also made a scattered light model unlikely.

Nebular continuum emission can probably be eliminated too: Dickson et al. (1995) suggest that nebular continuum emission should contribute a significant fraction of the UV flux from 4C41.17. The contribution of the nebular continuum is critically dependent on the mechanisms for Lyα production and suppression. Eales & Rawlings (1993) measure $F_{\text{Ly}\alpha} \approx 6F_{\text{H}\beta}$, compared to theoretical values of between 23 (for a thermal continuum) and ≈ 50 (for a hard ionising continuum) (Ferland & Osterbrock 1985). In the case that the low value of the line ratio is solely due to conventional dust extinction, and resonant scattering of Lyα photons is not important, this implies the true UV continuum flux should be 4-8 times its measured value, and, scaling the nebular continuum from Dickson et al. (1995), the contribution of that component to be $\approx 5 - 15$ per cent. The opposite case, when Lyα is suppressed solely by resonant scattering, and the extinction to the UV continuum is negligible, the contribution of the nebular continuum would be ≈ 50 per cent. However, if nebular continuum were to dominate the emission one might expect to see a steep *rise* towards shorter wavelengths across 912Å [the "Lyman break" in an optically thin nebular continuum spectrum (Landini & Monsignori-Fossi 1990)] unless the Lyα clouds are optically thick at the Lyman-limit when this radiation will be absorbed. Again, however, a high optical depth at the Lyman limit should produce very strong absorption in Lyα. Escape of Lyα photons from such clouds would be very inhibited if there were only a small amount of dust present in them.

The above discussion has served to highlight the problems associated with trying to understand the near-UV emission from high-z radio galaxies. In this case, it is however clear that Lyα observations at HST resolution could significantly improve the situation. They would allow the measurement of the Lyα flux from the compact UV-emitting regions in the centre of the galaxy, enabling the presence or absence of an HI screen between the UV-emitting region and the Lyα halo to be established. High-resolution imaging across the Lyman-limit break would also allow regions emitting optically-thin nebular continuum to be easily identified, although narrow band filters must be used to avoid interference by intervening absorbers.

ACKNOWLEDGEMENTS

REFERENCES

Beichmann C.A., 1987, ARA&A, 25, 521

Bithell M., 1991, MNRAS, 253, 320

Bruzual A. G., Charlot S., 1993, ApJ, 405, 538

Burstein D., Heiles C., 1982, AJ, 87, 1165

Cardelli J.A., Clayton G.C., Mathis J.S., 1989, ApJ, 345, 245

Chambers K.C., Miley G.K., van Breugel W.J.M., 1990, ApJ, 363, 21 (Ch90)

Chini R., Krügel E., 1994, A&A, 288, L33

Coleman G.D., Wu Chi-Chao, Weedman D.W., 1980, ApJS, 43, 393

Dickinson M., Spinrad H., Liebert J., 1991, Bull AAS, 23, 951

Dickson R., Tadhunter C., Shaw M., Clark N., Morganti R., 1995, MNRAS, 273, L29

Dunlop J.S., Hughes D.H., Rawlings S., Eales S.A., Ward M.J., 1994, Nat, 370, 347

Dunlop J.S., Guiderdoni B., Rocca-Volmerange B., Peacock J.A., Longair M.S., 1989, MNRAS, 240, 257

Eales S.A., Rawlings S., 1993, ApJ, 411, 67

Ellingson E., Yee H.K.C., Green R.F., 1991, ApJ, 371, 49

Ferland G.J., Osterbrock D.E., 1985, ApJ, 289, 105

Giavalisco M., Steidel C.C., Szalay A.S., 1994, ApJ, 425, L5

Graham J.R., Matthews K., Soifer B.T., Nelson J.E., Harrison W., Jernigan J.G., Lin S., Neugebauer G., Smith G., Ziomkowski C., 1994, ApJ, 420 L5 (G94)

Guhathakurta P., Tyson J.A., Majewski S.R., 1990, ApJ, 357, L9

Hill G.J., Lilly S.J., 1991, ApJ, 367, 1

Hippelein H., Meisenheimer K., 1993, Nat, 362, 224

King D.L., 1985, RGO Technical Note No. 31

Kron R.G., 1980, ApJS, 43, 305

Landholt A.U., 1992, AJ, 104, 340

Landini, M., Monsignori-Fossi B.C., 1990, A&AS, 82, 229

Lilly S.J., Cowie L.L., Gardner J.P., 1991, ApJ, 369, 79

Madau P., 1995, ApJ, 441, 18

Miley G.K., Chambers K.C., van Breugel W.J.M., Macchetto F., 1992, ApJ, 401, L69

Møller P., Jakobsen P., 1990, A&A, 228, 299

Rocca-Volmerange B., Guiderdoni B., 1988, A&AS, 75, 93

Schechter P., 1976, ApJ, 203, 297

Steidel C.C., Hamilton D., 1992, ApJ, 104, 941

Steidel C.C., Hamilton D., 1993, ApJ, 105, 2017

Steidel C.C., Pettini M., Hamilton D., 1995, AJ, in press

Storrie-Lombardi L.J., McMahon R.G., Irwin M.J., Hazard C., 1994, ApJ, 427, L13

Tyson J.A., 1988, AJ, 96, 1

Rawlings S., 1992, in Roland J., Sol H., Pelletier G., eds, Extragalactic Radio Sources – From Beams to Jets. Cambridge University Press, Cambridge, p. 332

Warren S.J., Hewett P.C., Osmer P.S., 1994, ApJ, 421, 412

Table 2. Magnitudes and colours of the objects in the 4C41.17 field

Object name	Structure with HST	R_{tot}	Aperture diameter /arcsec	R	ΔR	$V - R$	$\Delta(V - R)$	$U - V$	$\Delta(U - V)$	$R - K$	$\Delta(R - K)$	$K_S - K$	$\Delta(K_S - K)$	Notes
LR1	S	18.33	5	18.47	0.00	0.73	0.00	2.30	0.02	-	-	-	-	
LR2	-	21.53	4	21.53	0.01	0.33	0.01	0.17	0.02	-	-	-	-	
LR3	G?	24.02	2	24.59	0.09	0.95	0.17	-0.92	0.19	-	-	-	-	
LR4	G	22.18	3	22.70	0.02	1.07	0.04	>1.64		4.62	0.04	0.35	0.05	G94 object 1
LR5	S	21.07	3	21.35	0.01	0.75	0.01	2.26	0.08	3.55	0.01	0.15	0.01	G94 object 7
LR6	S	22.73	3	23.23	0.04	1.03	0.08	>1.14		3.45	0.08	0.07	0.09	G94 object 15
LR7	?	24.07	2	25.23	0.17	0.84	0.30	>-0.22		-		-		not detected by G94 ($K \geq 21.5$)
LR8	-	23.68	2	24.56	0.09	0.85	0.16	0.16	0.31	-		-		
LR9	G	21.56	3	22.48	0.01	0.39	0.02	>2.54		2.73	0.04	1.38	0.10	4C41.17
LR10	?	24.43	2	25.05	0.14	0.69	0.22	-0.97	0.22	-		-		not detected by G94 ($K \geq 21.5$)
LR11	G	24.24	3	24.05	0.09	>2.00	-	($U > 25.41$)		3.40	0.28	0.08	0.29	G94 object 3; Ch90 object 'w'
LR12	S	19.65	3	20.10	0.00	0.73	0.00	2.50	0.08	3.43	0.00	0.13	0.00	G94 object 13; Ch90 object 'y'
LR13	?	21.26	2	22.47	0.01	0.54	0.01	0.40	0.04	-		-		
LR14	G	24.76	3	24.26	0.17	1.17	0.41	>-0.02		5.85	0.17	0.16	0.04	G94 object 8
LR15a	G	20.95	2	22.32	0.01	0.82	0.02	1.33	0.10	4.39	0.03	-		
LR15b	G	(a+b)	2	23.23	0.03	0.79	0.05	-0.15	0.07	<2.74	-	-		
LR16	G	22.70	3	22.60	0.02	0.26	0.03	1.17	0.14	<2.55	-	-		
LR17	G	23.64	2	24.54	0.09	0.26	0.12	-0.29	0.14	4.59	0.24	-		
LR18	G?	23.88	2	24.65	0.10	0.03	0.12	0.31	0.17	<4.16	-	-		
LR19	-	23.78	2	24.19	0.06	0.78	0.11	>0.88		<3.70	-	-		
LR20	-	21.92	4	21.90	0.02	0.66	0.03	2.28	0.29	2.93	0.18	-		
LR21	G	23.69	2	25.06	0.14	0.18	0.18	>0.61		<4.57	-	-		

Notes: a flat-spectrum object has $V - R = 0.30$, $U - V = -0.77$ and $R - K = 1.94$. Errors are those from Poisson noise only, to these should be added errors of ~ 0.15 mag from the sky determination and ~ 0.15 mag from the absolute calibration. These have been excluded from the table as we are mostly concerned with relative photometry, in which small absolute flux scale errors are unimportant and errors in the sky determination are quite likely to be correlated between bands. The errors in total magnitudes are discussed in section 3. Dashes in the second column indicate that the object was off the HST field of Miley et al. (1992), queries indicate that the object was present, but too faint to be classified reliably.